HHS Public Access

Author manuscript

Kidney Int. Author manuscript; available in PMC 2019 December 01.

Published in final edited form as:

Kidney Int. 2018 December ; 94(6): 1151–1159. doi:10.1016/j.kint.2018.06.031.

Hydroxypropyl-β-cyclodextrin protects from kidney disease in experimental Alport syndrome and focal segmental glomerulosclerosis

Alla Mitrofanova, PhD[#1,2,3], **Judith Molina, PhD**[#1,2], **Javier Varona Santos, PhD**[1,2], **Johanna Guzman, MD**[1,2], **Ximena A. Morales, MD**[1,2], **Gloria Michelle Ducasa, BS**[1,2,4], **Jonathan Bryn**[1,2], **Alexis Sloan, PhD**[1,2], **Ion Volosenco, MD**[1,2], **Jin-Ju Kim, PhD**[1,2], **Mengyuan Ge, BS**[1,2,4], **Shamroop K. Malela, PhD**[1,2], **Matthias Kretzler, MD**[5], **Sean Eddy, PhD**[5], **Sebastian Martini, MD**[5], **Patricia Wahl, PhD**[1,2], **Santiago Pastori, MD**[1,2], **Armando J. Mendez, PhD**[6], **George W. Burke, MD**[3,6], **Sandra Merscher, PhD**[1,2], and **Alessia Fornoni, MD, PhD.**[1,2,*]

[1]Katz Family Division of Nephrology and Hypertension, Department of Medicine, University of Miami Miller School of Medicine, Miami, Florida

[2]Peggy and Harold Katz Family Drug Discovery Center, University of Miami Miller School of Medicine, Miami, Florida

[3]Departament of Surgery, University of Miami Miller School of Medicine, Miami, FL

[4]Department of Molecular and Cellular Pharmacology, University of Miami Miller School of Medicine, Miami, Florida

[5]Division of Nephrology, Departments of Internal Medicine and Computational Medicine and Bioinformatics, University of Michigan School of Medicine, Ann Arbor, Michigan

[6]Diabetes Research Institute, University of Miami Miller School of Medicine, Miami, Florida

[#] These authors contributed equally to this work.

[*] *Correspondence to:* Alessia Fornoni, MD, PhD, Katz Family Division of Nephrology and Hypertension and Peggy and Harold Katz Family Drug Discovery Center, University of Miami, Address: 1580 NW 10th Ave, Miami, FL 33136, USA, Tel: +1 305-243-3583, Fax: +1 305-243-3506, afornoni@med.miami.edu.

AUTHORSHIP

AM and JMD conceived the project, performed the in vitro and in vivo experiments, analyzed the data, and wrote the manuscript. JVS performed all in vitro experiments related to detection of total and esterified cholesterol and triglycerides in mice kidney cortexes. JG performed some in vivo and in vitro experiments on ADR treated mice. XAM performed some in vivo and vitro experiments on Alport mice. GMD, JB, AS, IV, JJK, MG SKM performed some of the in vitro experiments. MK, SE, SM performed and provided data on the human microarray analysis. PW, SP analyzed microarray experimental data. AJM designed experiments related to cholesterol determination and cholesterol efflux. GWB conceived one of the techniques utilized. SM and AF conceived the project, designed and supervised the study, analyzed the data, and edited the manuscript. AF is the guarantor of this work and, as such, had full access to all the data in the study and takes responsibility for the integrity of the data and the accuracy of the data analysis.

DISCLOSURE

G.W.B., A.F., and S.M. are inventors on pending or issued patents aimed to diagnose or treat proteinuric renal diseases. They stand to gain royalties from their future commercialization. A.F. is Chief Scientific Officer of L&F Health LLC and is consultant for Variant Pharmaceutical. Variant Pharmaceuticals, Inc. has licensed worldwide rights to develop and commercialize hydroxypropyl-beta-cyclodextrin for treatment of kidney disease from L&F Research. S.M. holds equity interest in a company presently commercializing the form of cyclodextrin referenced in this paper.

Abstract

Studies suggest that altered renal lipid metabolism plays a role in the pathogenesis of diabetic kidney disease and that genetic or pharmacological induction of cholesterol efflux protects from the development of diabetic kidney disease and focal segmental glomerulosclerosis (FSGS). Here we tested whether altered lipid metabolism contributes to renal failure in the Col4a3 knockout mouse model for Alport Syndrome. There was an eight fold increase in the cholesterol content in renal cortexes of mice with Alport Syndrome. This was associated with increased glomerular lipid droplets and cholesterol crystals. Treatment of mice with Alport Syndrome with hydroxypropyl-β-cyclodextrin (HPβCD) reduced cholesterol content in the kidneys of mice with Alport Syndrome and protected from the development of albuminuria, renal failure, inflammation and tubulointerstitial fibrosis. Cholesterol efflux and trafficking related genes were primarily affected in mice with Alport Syndrome and were differentially regulated in the kidney cortex and isolated glomeruli. HPβCD also protected from proteinuria and mesangial expansion in a second model of non-metabolic kidney disease; adriamycin-induced nephropathy. Consistent with our experimental findings, microarray analysis confirmed dysregulation of several lipid related genes in glomeruli isolated from kidney biopsies of patients with primary FSGS enrolled in the NEPTUNE study. Thus, lipid dysmetabolism occurs in non-metabolic glomerular disorders such as Alport Syndrome and FSGS, and HPβCD improves renal function in experimental Alport Syndrome and FSGS.

Keywords

Cholesterol metabolism; FSGS, Alport syndrome; renal function; hydroxypropyl beta cyclodextrin

INTRODUCTION

Recent research suggests that renal rather than systemic dyslipidemia contributes to the pathogenesis and progression of kidney diseases[1–5], similarly to what was described for atherosclerosis[6–10] and non-alcoholic fatty liver disease[11–13]. Glomerular cholesterol accumulation was reported in experimental models of type 1 and type 2 diabetes[2, 4, 14] and in patients with type 2 diabetic kidney disease (T2DKD)[1]. In these studies, genes involved in reverse cholesterol transport (RCT) were significantly modulated in glomeruli, and gene expression correlated with eGFR. These findings are consistent with our published data indicating that ATP-binding cassette transporter (ABCA1) expression is reduced in glomeruli of patients with T2DKD[2] and that impaired ABCA1-mediated RCT occurs in a mouse model of focal segmental glomerulosclerosis (FSGS) developed by us where podocyte injury and development of chronic kidney disease (CKD) were rescued by ABCA1 transgene expression or treatment with Hydroxypropyl-β-cyclodextrin (HPβCD)[3]. These observations challenge the concept that lipoid nephrosis is a consequence of the hyperlipidemia associated with nephrotic syndrome development and disease progression and suggest that lipid accumulation in glomerular cells may instead contribute to disease pathogenesis.

Consistent with this hypothesis, genetic diseases such as Tangier Disease[15], LCAT deficiency[16–19] and Niemann-Pick Type C disease[20] also display cholesterol accumulation in peripheral organs, which contributes to the clinical manifestations. To a certain degree,

proteinuria, foamy podocytes and nephrotic syndrome are associated with these genetic disorders suggesting that altered cholesterol homeostasis (CH) may contribute to the development of glomerular diseases. Additionally, an important role of apolipoprotein A-I (APOAI) in the pathogenesis of nephrotic syndrome has been reported[21], and APOAI variants were shown to play an important role in the recurrence of proteinuria after transplantation in FSGS patients[22].

The objective of the present study was to determine if dysregulation of cellular lipid homeostasis can be observed in clinical and experimental non-metabolic glomerular diseases and to evaluate whether the protective effect of HPβCD as previously described by us in the FSGS NFAT mouse model[3] can also be observed in experimental models of AS and in a second, less progressive model of Adriamycin-induced nephropathy, a model of FSGS[23–25].

RESULTS

Esterified and free cholesterol accumulation occurs in kidney cortexes in an experimental Alport Syndrome (AS) nephropathy.

We first aimed at determining if glomerular lipid accumulation is associated with renal dysfunction in Col4a3 knockout mice (AS mice) as a model for AS nephropathy, similarly to what we previously described in experimental DKD[2]. We show that AS mice are characterized by renal cholesterol ester accumulation (Figure 1A) in the absence of changes in total kidney cholesterol (Figure 1B) content when compared to wildtype mice. Additionally, we detected cholesterol crystal accumulation in AS mice compared to wildtype littermates (Figure 1C) similarly to what was described in atherosclerosis[26, 27] indicating that both free and esterified cholesterol accumulation occurs in kidneys of mice with AS and may contribute to the pathogenesis of the disease. However, the exact mechanisms by which dysregulation of CH may cause lipotoxicity warrants further investigation.

HPβCD prevents proteinuria and renal function decline and prolongs survival in experimental AS nephropathy.

We then investigated the potential beneficial effect of HPβCD in preserving renal function in another experimental model of non-diabetic kidney disease (NDKD) in AS mice. AS mice were subcutaneously injected with HPβCD (4000 mg/kg) three times per week and compared to untreated controls. We detected a decrease in the albumin-to-creatinine ratio (ACR) in AS mice treated with HPβCD (Figure 2A). More importantly, a drastic decrease of BUN (Figure 2B) and serum creatinine levels (Figure 2C) was observed. HPβCD treatment also reduced mesangial expansion (Figure 2D, E). Picrosirius red staining of kidney sections indicated increased fibrosis in AS mice which was reduced by treatment with HPβCD (Figure 2F, G). Moreover, electron microscopy analysis revealed significant improvement of podocyte foot processes effacement (Figure 2H, I) in the absence of changes in glomerular basement membrane thickness (Figure 2J) in AS mice treated with HPβCD compared to AS mice injected with saline solution. Finally, HPβCD treatment extended the lifespan of AS mice by about 22% compared to untreated mice (Figure 2K). Histological analysis of skin at the HPβCD injection site showed preserved histology and no inflammatory infiltrate

(Supplementary Figure 1). These data indicate that HPβCD prevents renal function decline in AS mice and suggest that this may occur by lowering cellular lipid content.

HPβCD affects renal lipid accumulation in experimental AS.

To investigate if HPβCD prevents cholesterol ester and crystal accumulation in kidneys of AS mice, Oil Red O staining was performed on kidney sections of AS mice. We found increased neutral lipid accumulation in AS mice compared to controls which was reduced by HPβCD (Figure 3A, B). Reduced lipid accumulation was associated with reduced cholesterol ester accumulation in AS mice four weeks after HPβCD administration (Figure 3C), whereas total cholesterol (Figure 3D) level remained unchanged. Finally, HPβCD also prevented cholesterol crystal accumulation (Figure 3E, F) in kidney cortexes of AS mice. HPβCD did restore normal cellular CH and raised serum HDL levels while LDL and cholesterol levels remained unchanged (Table 1). These data indicate that HPβCD may prevent renal function decline in AS mice by lowering the cellular lipid content and/or affecting serum HDL.

QRT-PCR demonstrates impaired RCT in glomeruli of mice with AS.

We previously reported reduced ABCA1 expression in glomeruli of patients with T2DKD[2] as well as accumulation of cholesterol in kidney cortexes in experimental diabetic kidney disease (DKD) and in a mouse model of focal segmental glomerulosclerosis (FSGS)[3]. We therefore investigated Abca1 and Abcg1 expression was reduced in mRNA isolated from glomeruli of 4, 6, and 8 weeks old AS mice. We found that both Abca1 and Abcg1 expression were significantly decreased in early stages of disease progression (Figure 4A, B). These data suggest that in experimental AS impaired glomerular RCT may contribute to the development of renal failure. Impaired RCT seems to be specific to glomeruli, as a different and opposite regulation of genes involved in RCT was observed by QRT-PCR when expression in whole kidney cortex was analyzed (Supplementary Figure 2).

HPβCD protects from experimental FSGS.

To further support our previous study which indicated a therapeutic effect of HPβCD in experimental FSGS (NFAT mouse model)[3], we used a second, well-established experimental model for FSGS, mice with Adriamycin (ADR)-induced nephropathy[28]. These mice are characterized by a milder, less progressive form of nephropathy when compared to the NFAT mouse model. To validate the therapeutic effect of HPβCD in this model, five-week old BALB/c mice were injected with one dose of ADR (11 mg/kg). Twenty-four hours later, HPβCD (40 mg/kg) was delivered via subcutaneous osmotic pump for 10 weeks. Decreases in the albumin/creatinine ratio (ACR) (Figure 5A) and blood urea nitrogen (BUN) (Figure 5B) were observed in the HPβCD treated mice after 10 weeks of treatment compared to untreated mice (CTRL), whereas serum creatinine levels remained unchanged (Figure 5C). Histological analysis of kidney sections confirmed a protective effect of HPβCD on glomerular injury as indicated by a reduction of the glomerular area exhibiting mesangial expansion (Figure 5D, E). Taken together, these data indicate that HPβCD protects from the development of renal disease in a second model of non-metabolic glomerular disease, ADR induced nephropathy.

Genes regulating cholesterol homeostasis (CH) are differentially expressed in glomeruli patients affected by primary FSGS.

To determine if the dysregulation of genes important in regulating cellular lipid homeostasis can be observed in these glomerular diseases of non-metabolic origin, microarray analysis of mRNA isolated from glomerular compartments microdissected from kidney biopsies of FSGS patients enrolled in the NEPTUNE study was performed. We found that twenty-one out of forty-six key genes regulating cholesterol homeostasis and selected by us for further analysis (Supplementary Table 1) were differentially expressed in glomeruli of FSGS patients compared to control living donors (Figure 6). Differentially expressed genes included those regulating cholesterol influx (LDLR, NR1H2), synthesis (HMGCR, SREBF2, SCAP), efflux (ABCA1, ABCG1, APOC3, APOL1, APOM) and cholesterol trafficking and esterification (CETP, GPBAR1, NPC1, SOAT1). Interestingly, all but two genes, APOC3 and APOM, were upregulated in glomeruli of FSGS patients. Although a reduction in ABCA1 expression was not observed, these results support a hypothesis that dysregulation of genes regulating CH contributes to the pathogenesis of clinical FSGS.

DISCUSSION

Our study was designed to test if dysregulation of glomerular CH is a common mechanism that contributes to the pathogenesis of glomerular diseases of non-metabolic origin and if HPβCD represents a potential therapeutic option to prevent disease progression in these conditions.

Our findings suggest that lipotoxicity may contribute to the pathogenesis of glomerular diseases of non-metabolic origin. First, we showed that cholesterol ester and/or crystal accumulation occurs in glomeruli of AS mice suggesting that chronic kidney disease may represent a form of fatty kidney disease. Second, we found that HPβCD protects AS mice against the development of proteinuria, progressive renal failure and fibrosis. In addition, HPβCD treatment resulted in improved survival. Similarly, HPβCD protected mice with ADR induced nephropathy from proteinuria, increased BUN and mesangial expansion. Moreover, we determined the protective effect of HPβCD on kidney damage in AS mice was associated with a protection from lipid accumulation and found that HPβCD reduced renal cholesterol ester, lipid droplet, and cholesterol crystal content. These data support our previous study which indicated a preventive effect of HPβCD in the progression of DKD[2] and in a newly established model of experimental FSGS (NFAT mouse model)[3]. Findings from others showed that HPβCD promotes the regression of atherosclerosis[29] and exercises neuroprotective effects in experimental models of Niemann-Pick C disease[30], including ongoing clinical trials for the treatment of Niemann-Pick C disease, and Alzheimer disease[31]. Third, we validated our observations obtained in AS mice by demonstrating that genes important in regulating CH are differentially expressed in glomeruli from patients with FSGS enrolled in the NEPTUNE cohort.

Consistent with our prior findings in clinical and experimental DKD[2], the expression of Abca1 and Abcg1 was significantly decreased in glomeruli of mice with AS at early stages of disease. This observation indicated that in AS cholesterol accumulation due to impaired RCT in glomeruli occurs concomitantly with the development of renal failure and may

contribute to the pathogenesis and/or progression of kidney disease. Nevertheless, the exact mechanisms as to how the dysregulation of ABCA1 and ABCG1 as well as other genes important in regulating RCT in other structures of the kidney cortex, such as in the tubules, contributes to disease pathogenesis and/or progression in AS warrants further investigation, as ABCA1, ABCG1 and other genes involved in cholesterol efflux were indeed upregulated when mRNA analysis were performed in whole kidney cortex.

In order to clinically validate altered CH in glomerular diseases of non-metabolic origin, we interrogated glomerular gene expression datasets from FSGS patients (NEPTUNE) for differential gene expression of forty-five lipid related genes and identified twenty-two genes that were modulated in FSGS when compared to healthy living donors. Interestingly, genes regulating cholesterol influx (LDLR), synthesis (HMGCR) and a master regulator of the cholesterol pathway, SREBF2, were found strongly upregulated, indicating that cholesterol accumulation also contributes to the pathogenesis of clinical FSGS but possibly through a more complex modulation involving several pathways important in CH. However, as the glomerular expression of ABCA1 and ABCG1 was not affected in clinical FSGS, it is possible that different mechanisms contribute to lipid accumulation in experimental and clinical FSGS. Alternatively, as the kidney biopsies in NEPTUNE patients were done at disease onset, it is possible that the downregulation of ABCA1 and ABCG1 occurs at a later stage and contributes to disease progression or that the heterogeneity of this study population was responsible for this negative result.

In conclusion, our study suggests that renal cholesterol accumulation due to impaired RCT in experimental models of non-metabolic glomerular disorders might contribute to renal cholesterol accumulation, proteinuria and, in the case of AS, to a progressive decline in renal function. Similarly to what we observed for experimental DKD where ABCA1/APOA1 mediated RCT is impaired and seems to be the driving pathogenic factor, impaired glomerular ABCA1/APOA1 mediated RCT may also to be a key contributing factor in AS. While some concerns on HPβCD ototoxicity have been raised[32], our data suggest that HPβCD treatment could overcome the effect of cholesterol mediated toxicity in renal cells and prevent renal failure.

METHODS

Microarray analysis.

The institutional review board and ethics committee approved this research protocol. Kidney biopsies were obtained from 48 patients with biopsy proven FSGS from the NEPTUNE study (NCT01209000) and 6 healthy living donors controls[33]. Glomerular compartments of the kidney biopsy tissue specimens were manually microdissected and mRNA was isolated as previously described[34, 35]. Glomerular gene expression profiling was performed using Human Genome ST2.1 Affymetrix Gene Chip arrays was processed using a modified affy package in R[36], with custom CDF annotations applied such that a single gene is represented by a single probe set (ENTREZG v19, brainarray.mbni.med.umich.edu)[37]. Differential expression analysis of glomerular transcripts between control and disease group was performed using Significance Analysis of Microarray (SAM) as implemented in the TIGR

Multiexperiment Viewer software suite. Forty-five genes involved in lipid metabolism were selected and included in this study (Supplementary Table 1).

Animal studies.

All animal procedures were conducted under protocols approved by the Institutional Animal Care and Use Committee at the University of Miami. Col4a3 knockout mice were used as a model of AS (129-Col4a3^{tm1Dec}/J, #002908, Jackson Laboratories, USA). Four-week-old female Col4a3 knockout (Col43−/−) and Col4a3 wildtype (Col4a3+/+) mice were injected subcutaneously with ready-to-use hydroxypropyl-β-cyclodextrin solution (HPβCD)(CTD Inc., FL) or 0.9% saline solution (NS) (Teknova, CA). HPβCD (4000 mg/kg) was administered subcutaneously 3-times per week for 4 weeks as described by us[2]. ADR nephropathy was induced by a single intravenous Adriamycin (11 mg/kg) injection (Sigma-Aldrich, MO) followed 24 hours later by subcutaneous administration of HPβCD (40 mg/kg, Sigma Aldrich, MO) using osmotic pumps (Alzet 2004, 0.25 μl/hr, Alzet, CA) for 10 weeks. Four groups of five-week-old BALB/c mice were utilized: control (n=6), ADR injected (n=6), HPβCD treated (n=6), and mice injected with ADR and HPβCD (n=6). Urines were collected, body weight was determined weekly. Ten weeks after treatment initiation, kidneys were harvested for further analysis as previously described[2]. Blood samples were collected and analyzed for serum cholesterol, triglycerides, HDL, VLDL and blood urea nitrogen (BUN) levels in the Comparative Laboratory Core Facility (University of Miami). Serum creatinine was determined by tandem mass spectrometry at the UAB-UCSD O'Brien Core Center (University of Alabama at Birmingham) as previously described[38]. The urine albumin content was measured by ELISA (Bethyl Laboratories, TX). The urine creatinine content was assessed by an assay based on the Jaffe method (Stanbio Laboratory, USA). Albumin/creatinine ratio (ACR) values were calculated and expressed as microgram albumin per milligram creatinine.

Quantitative real-time PCR.

mRNA from kidney cortexes of Col4a3 knockout mice was extracted using RNAspin Mini kit (GE Healthcare, USA). Reverse transcription was performed and relative gene expression was determined as previously described by us[2, 3]. Primers used are listed in Supplementary Table 2.

Cholesterol content determination.

Briefly, tissue from kidney cortexes was homogenized in hypotonic buffer (10mM HEPES pH7.0, 15mM KCl, 1mM $MgCl_2$, 10mM phosphatase inhibitors). Lipids from 100μl of the homogenate were extracted and cholesterol content was determined using the Amplex Red Cholesterol Assay Kit (ThermoFisher Scientific, MA) following the manufacturer's instructions. Cholesteryl ester (CE) quantification was performed as previously described[39].

Histology and assessment of mesangial expansion.

Periodic acid-Schiff (PAS) staining of 4μm-thick tissue sections was performed using a standard protocol. Twenty glomeruli per section were analyzed for mesangial expansion by semi quantitative analysis (scale 0–4) performed by two blinded independent investigators.

Oil red O staining.

Filtered Oil-Red O-Isopropanol solution (Electron Microscopy Science, PA) was diluted with water (6:4). 4μm kidney sections were incubated with 100μl freshly prepared Oil-Red solution for 15 minutes and counterstained with Hematoxylin Harris Hg Free (VWR, PA) to detect lipid deposition. Glomeruli staining was evaluated using a light microscope (Olympus BX 41, Tokyo, Japan)[40].

Transmission electron microscopy and measurement of foot processes effacement and glomerular basement membrane thickness.

For ultrastructural analyses, samples were fixed in 4% paraformaldehyde/1% glutaraldehyde (Boston BioProducts, MA, USA) in 100 mM phosphate buffer, pH 7.2 for 2 h at room temperature and then overnight at 4°C. Samples were then rinsed extensively in dH20 prior to en bloc staining with 1% aqueous uranyl acetate (Ted Pella Inc., Redding, CA, USA) for 1 hr. Following several rinses in dH20, samples were dehydrated in a graded series of ethanol and embedded in Eponate 12 resin (Ted Pella Inc., USA). Sections of 95 nm were cut with a Leica Ultracut UCT ultramicrotome (Leica Microsystems Inc., Bannockburn, IL, USA), stained with uranyl acetate and lead citrate, and viewed on a JEOL 1200 EX transmission electron microscope (JEOL USA Inc., Peabody, MA, USA) equipped with an AMT 8 megapixel digital camera and AMT Image Capture Engine V602 software (Advanced Microscopy Techniques, Woburn, MA, USA). Electron micrographs were captured at 10,000x magnification. Eight images per mouse were analyzed using the distance between two points on a ruler of a photograph as a measurement scale. Glomerular basement membrane (GBM) thickness was measured in thirty different points. The number of podocyte foot processes (FP) along the GBM was counted by hand. A FP was defined as any connected epithelial segment butting on the basement membrane, between two neighboring filtration pores or slits.

Cholesterol crystal detection.

TissueTek OCT (VWR, PA, USA) embedded kidney sections (4 μm) were used to detect cholesterol crystals. Cryosections were stained with hematoxylin (VWR, PA, USA) for 5 min and then mounted with glycerol 10%. Crystal area was visualized using polarized light microscope (Olympus BX 41, Tokyo, Japan) at 40x magnification[41].

Statistical analysis.

Data are expressed as a mean ± standard deviation (SD). A number of experiments ranging between 3 and 5 was utilized as indicated for each distinct experiment. Minimal group sizes for in vitro and in vivo studies were determined via power calculator using the DSS Researcher's Toolkit with an α of 0.05. Animals were grouped unblinded, but randomized, and investigators were blinded for the quantification experiments. GraphPad Prism Outlier calculator software (https://www.graphpad.com/quickcalcs/Grubbs1.cfm) was used to indicate outliers in each set of data obtained for in vitro and in vivo experiments. Significant outliers were excluded from further statistical analysis. Two groups of data were compared using the two-tailed t-test. Three and more groups of data were compared using the One-Way analysis of variance (ANOVA), followed by Tukey's post-test or Two-Ways ANOVA

with multiple comparisons. $p<0.05$ was taken to indicate statistical significance. Statistical analysis was performed using the GraphPad Prism, version 5.0 (GraphPad Software Inc.).

Supplementary Material

Refer to Web version on PubMed Central for supplementary material.

ACKNOWLEDGMENTS

AF is supported by the NIH grants DK090316, DK104753, U24DK076169, U54DK083912, UM1DK100846, and 1UL1TR000460. AF, SM, CF are supported by Hoffman-La Roche. GMD is supported by a Predoctoral Fellowship of the American Heart Association (16PRE30200010).

The Nephrotic Syndrome Study Network Consortium (NEPTUNE), U54-DK-083912, is a part of the National Institutes of Health (NIH) Rare Disease Clinical Research Network (RDCRN), supported through a collaboration between the Office of Rare Diseases Research (ORDR), NCATS, and the National Institute of Diabetes, Digestive, and Kidney Diseases. Additional funding and/or programmatic support for this project has also been provided by the University of Michigan, the NephCure Kidney International and the Halpin Foundation.

REFERENCES

1. Herman-Edelstein M, Scherzer P, Tobar A, et al. Altered renal lipid metabolism and renal lipid accumulation in human diabetic nephropathy. Journal of lipid research 2014; 55: 561–572. [PubMed: 24371263]
2. Merscher-Gomez S, Guzman J, Pedigo CE, et al. Cyclodextrin protects podocytes in diabetic kidney disease. Diabetes 2013; 62: 3817–3827. [PubMed: 23835338]
3. Pedigo CE, Ducasa GM, Leclercq F, et al. Local TNF causes NFATc1-dependent cholesterol-mediated podocyte injury. The Journal of Clinical Investigation 2016; 126: 3336–3350. [PubMed: 27482889]
4. Wang Z, Jiang T, Li J, et al. Regulation of renal lipid metabolism, lipid accumulation, and glomerulosclerosis in FVBdb/db mice with type 2 diabetes. Diabetes 2005; 54: 2328–2335. [PubMed: 16046298]
5. Kang HM, Ahn SH, Choi P, et al. Defective fatty acid oxidation in renal tubular epithelial cells has a key role in kidney fibrosis development. Nat Med 2015; 21: 37–46. [PubMed: 25419705]
6. Brown MS, Goldstein JL. Lipoprotein metabolism in the macrophage: implications for cholesterol deposition in atherosclerosis. Annu Rev Biochem 1983; 52: 223–261. [PubMed: 6311077]
7. Libby P, Ridker PM, Maseri A. Inflammation and atherosclerosis. Circulation 2002; 105: 1135–1143. [PubMed: 11877368]
8. den Hartigh LJ, Connolly-Rohrbach JE, Fore S, et al. Fatty acids from very low-density lipoprotein lipolysis products induce lipid droplet accumulation in human monocytes. J Immunol 2010; 184: 3927–3936. [PubMed: 20208007]
9. Swirski FK, Libby P, Aikawa E, et al. Ly-6Chi monocytes dominate hypercholesterolemia-associated monocytosis and give rise to macrophages in atheromata. J Clin Invest 2007; 117: 195–205. [PubMed: 17200719]
10. Wu H, Gower RM, Wang H, et al. Functional role of CD11c+ monocytes in atherogenesis associated with hypercholesterolemia. Circulation 2009; 119: 2708–2717. [PubMed: 19433759]
11. Ioannou GN. The Role of Cholesterol in the Pathogenesis of NASH. Trends Endocrinol Metab 2016; 27: 84–95. [PubMed: 26703097]
12. Ma KL, Ruan XZ, Powis SH, et al. Inflammatory stress exacerbates lipid accumulation in hepatic cells and fatty livers of apolipoprotein E knockout mice. Hepatology 2008; 48: 770–781. [PubMed: 18752326]
13. Puri P, Baillie RA, Wiest MM, et al. A lipidomic analysis of nonalcoholic fatty liver disease. Hepatology 2007; 46: 1081–1090. [PubMed: 17654743]

14. Jiang T, Liebman SE, Lucia MS, et al. Role of altered renal lipid metabolism and the sterol regulatory element binding proteins in the pathogenesis of age-related renal disease. Kidney Int 2005; 68: 2608–2620. [PubMed: 16316337]
15. Katz SS, Small DM, Brook JG, et al. The storage lipids in Tangier disease. A physical chemical study. J Clin Invest 1977; 59: 1045–1054. [PubMed: 193870]
16. Franco M, Castro G, Romero L, et al. Decreased activity of lecithin:cholesterol acyltransferase and hepatic lipase in chronic hypothyroid rats: implications for reverse cholesterol transport. Mol Cell Biochem 2003; 246: 51–56. [PubMed: 12841343]
17. Julve-Gil J, Ruiz-Perez E, Casaroli-Marano RP, et al. Free cholesterol deposition in the cornea of human apolipoprotein A-II transgenic mice with functional lecithin: cholesterol acyltransferase deficiency. Metabolism 1999; 48: 415–421. [PubMed: 10206431]
18. Tomimoto S, Tsujita M, Okazaki M, et al. Effect of probucol in lecithin-cholesterol acyltransferase-deficient mice: inhibition of 2 independent cellular cholesterol-releasing pathways in vivo. Arterioscler Thromb Vasc Biol 2001; 21: 394–400. [PubMed: 11231919]
19. Jimi S, Uesugi N, Saku K, et al. Possible induction of renal dysfunction in patients with lecithin:cholesterol acyltransferase deficiency by oxidized phosphatidylcholine in glomeruli. Arterioscler Thromb Vasc Biol 1999; 19: 794–801. [PubMed: 10073988]
20. Bi X, Liao G. Cholesterol in Niemann-Pick Type C disease. Sub-cellular biochemistry 2010; 51: 319–335. [PubMed: 20213549]
21. Vaziri ND, Kim HJ, Moradi H, et al. Amelioration of nephropathy with apoA-1 mimetic peptide in apoE-deficient mice. Nephrol Dial Transplant 2010; 25: 3525–3534. [PubMed: 20488818]
22. Lopez-Hellin J, Cantarell C, Jimeno L, et al. A form of apolipoprotein a-I is found specifically in relapses of focal segmental glomerulosclerosis following transplantation. Am J Transplant 2013; 13: 493–500. [PubMed: 23205849]
23. Wang Y, Wang YP, Tay YC, et al. Progressive adriamycin nephropathy in mice: sequence of histologic and immunohistochemical events. Kidney international 2000; 58: 1797–1804. [PubMed: 11012915]
24. Yoo TH, Pedigo CE, Guzman J, et al. Sphingomyelinase-like phosphodiesterase 3b expression levels determine podocyte injury phenotypes in glomerular disease. Journal of the American Society of Nephrology : JASN 2015; 26: 133–147. [PubMed: 24925721]
25. Cosgrove D, Meehan DT, Grunkemeyer JA, et al. Collagen COL4A3 knockout: a mouse model for autosomal Alport syndrome. Genes & development 1996; 10: 2981–2992. [PubMed: 8956999]
26. Janoudi A, Shamoun FE, Kalavakunta JK, et al. Cholesterol crystal induced arterial inflammation and destabilization of atherosclerotic plaque. Eur Heart J 2016; 37: 1959–1967. [PubMed: 26705388]
27. Tangirala RK, Jerome WG, Jones NL, et al. Formation of cholesterol monohydrate crystals in macrophage-derived foam cells. Journal of lipid research 1994; 35: 93–104. [PubMed: 8138726]
28. Lee VW, Harris DC. Adriamycin nephropathy: a model of focal segmental glomerulosclerosis. Nephrology (Carlton, Vic) 2011; 16: 30–38.
29. Zimmer S, Grebe A, Bakke SS, et al. Cyclodextrin promotes atherosclerosis regression via macrophage reprogramming. Science translational medicine 2016; 8: 333ra350.
30. Davidson CD, Ali NF, Micsenyi MC, et al. Chronic cyclodextrin treatment of murine Niemann-Pick C disease ameliorates neuronal cholesterol and glycosphingolipid storage and disease progression. PloS one 2009; 4: e6951. [PubMed: 19750228]
31. Yao J, Ho D, Calingasan NY, et al. Neuroprotection by cyclodextrin in cell and mouse models of Alzheimer disease. The Journal of experimental medicine 2012; 209: 2501–2513. [PubMed: 23209315]
32. Crumling MA, King KA, Duncan RK. Cyclodextrins and Iatrogenic Hearing Loss: New Drugs with Significant Risk. Frontiers in Cellular Neuroscience 2017; 11.
33. Gadegbeku CA, Gipson DS, Holzman LB, et al. Design of the Nephrotic Syndrome Study Network (NEPTUNE) to evaluate primary glomerular nephropathy by a multidisciplinary approach. Kidney international 2013; 83: 749–756. [PubMed: 23325076]
34. Saeed AI, Sharov V, White J, et al. TM4: a free, open-source system for microarray data management and analysis. BioTechniques 2003; 34: 374–378. [PubMed: 12613259]

35. Saeed AI, Bhagabati NK, Braisted JC, et al. TM4 microarray software suite. Methods in enzymology 2006; 411: 134–193. [PubMed: 16939790]

36. Gautier L, Cope L, Bolstad BM, et al. affy--analysis of Affymetrix GeneChip data at the probe level. Bioinformatics (Oxford, England) 2004; 20: 307–315.

37. Dai M, Wang P, Boyd AD, et al. Evolving gene/transcript definitions significantly alter the interpretation of GeneChip data. Nucleic acids research 2005; 33: e175. [PubMed: 16284200]

38. Takahashi N, Boysen G, Li F, et al. Tandem mass spectrometry measurements of creatinine in mouse plasma and urine for determining glomerular filtration rate. Kidney international 2007; 71: 266–271. [PubMed: 17149371]

39. Mizoguchi T, Edano T, Koshi T. A method of direct measurement for the enzymatic determination of cholesteryl esters. Journal of lipid research 2004; 45: 396–401. [PubMed: 14563821]

40. Mehlem A, Hagberg CE, Muhl L, et al. Imaging of neutral lipids by oil red O for analyzing the metabolic status in health and disease. Nature protocols 2013; 8: 1149–1154. [PubMed: 23702831]

41. Montes GS. Structural biology of the fibres of the collagenous and elastic systems. Cell biology international 1996; 20: 15–27. [PubMed: 8936403]

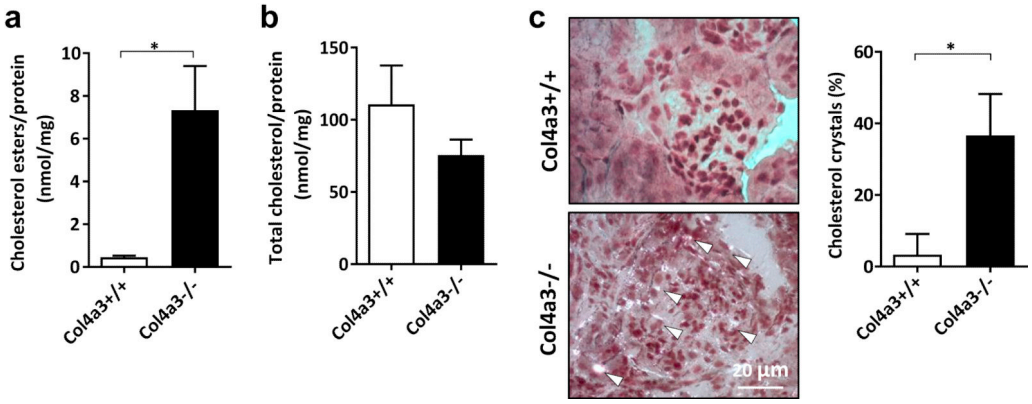

Figure 1. Cholesterol accumulation in kidney cortexes of Col4a3 knockout mice.

(A) Bar graph analysis showing significant accumulation of cholesterol esters in kidney cortexes of Col4a3 knockout mice compared to wildtype controls. *p<0.05, t-test. **(B)** No changes in total cholesterol levels are detected in kidney cortexes between Col4a3 knockout mice and wildtype littermates. *p<0.05, t-test. **(C)** Cholesterol crystal staining of kidney sections and bar graph analysis reveal significant cholesterol crystals accumulation (white arrows) in Col4a3 knockout mice (Col4a3−/−) when compared to wildtype littermates (Col4a3+/+). Bars are 20µm. *p<0.05, t-test. All data are presented as mean ± SD.

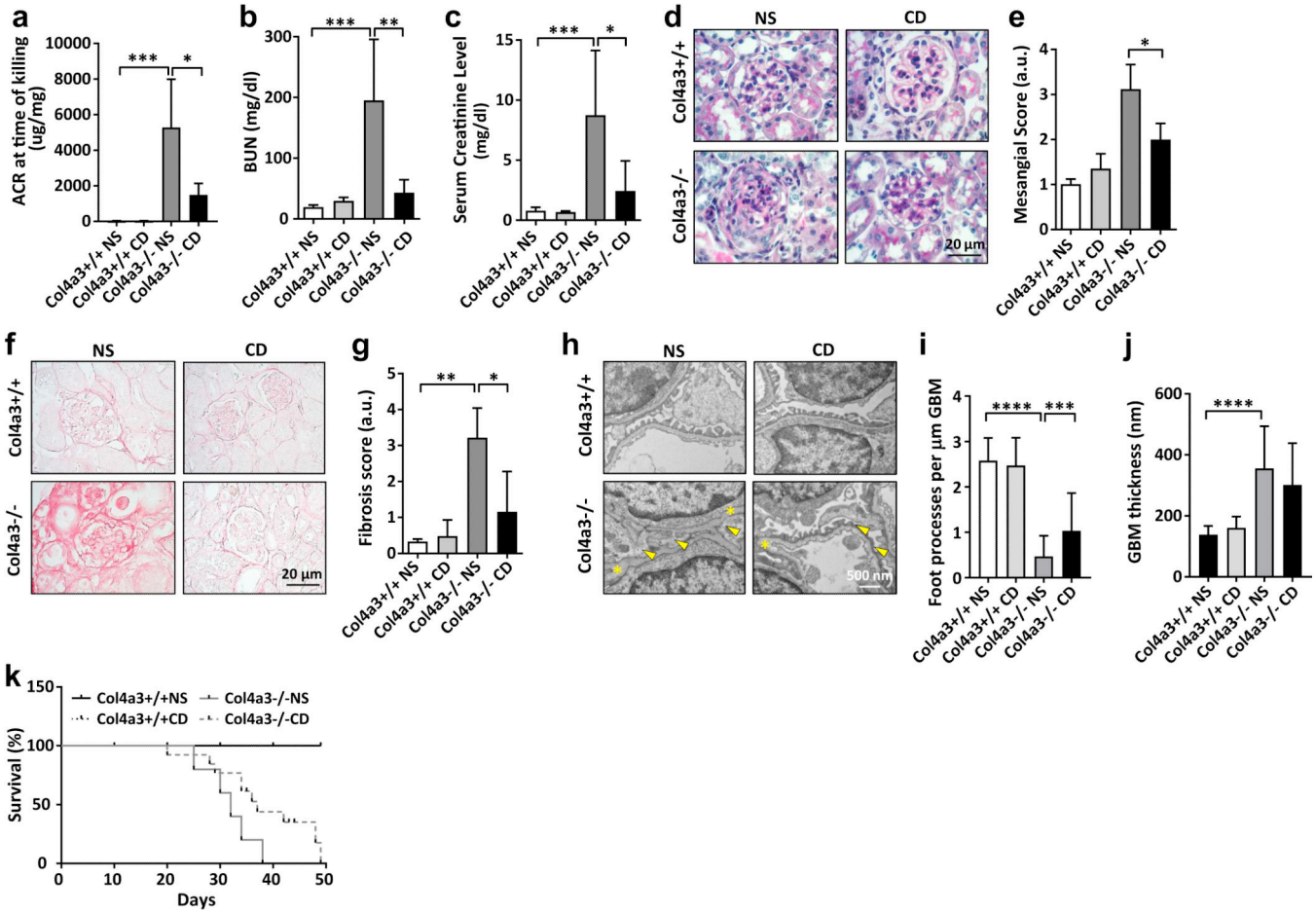

Figure 2. Hydroxypropyl-β–Cyclodextrin (HPβCD) improves the renal function in Col4a3 knockout mice.

Col4a3 knockout mice (Col43−/−) and wildtype littermates (Col4a3+/+) were injected subcutaneously with hydroxypropyl-β-cyclodextrin solution (HPβCD) at a dosage of 4000 mg/kg or with 0.9% saline solution (NS). Four groups of mice were analyzed: Col4a3+/+ NS (n=4), Col4a3+/+ CD (n=5), Col4a3−/− NS (n=4), and Col4a3−/− CD (n=4). All data are presented as mean ± SD. **(A)** CD treatment of Col4a3 knockout mice results in a reduction in the albumin/creatinine ratio (ACR). *p<0.05; ***p<0.001, t-test. **(B)** Bar graph analysis showing that serum BUN levels are significantly increased in Col4a3 knockout mice compared to wildtype littermates whereas HPβCD treatment prevents increases in serum BUN levels in Col4a3 knockout mice. **p<0.005, ***p<0.01, One-Way ANOVA. **(C)** Serum creatinine levels are increased in Col4a3 knockout mice compared to controls. HPβCD treatment results in reduction of the serum creatinine levels. *p<0.05, ***p<0.01, One-Way ANOVA. **(D)** Representative Periodic Acid-Schiff staining of kidney sections (4 µm) in Col4a3 knockout mice (40x). Bars are 20 µm. **(E)** Bar graph analysis of the scores for mesangial expansion after 4 weeks of treatment with HPβCD. Quantification was performed by two blinded, independent investigators. HPβCD treatment significantly reduces mesangial expansion in Col4a3 knockout mice. *p<0.05, One-Way ANOVA. **(F)** Representative Picrosirius Red (PSR) staining of kidney sections (4 µm) in Col4a3 knockout

mice (40x). Bars are 20 μm. **(G)** Bar graph analysis of PSR staining demonstrates increased fibrosis in Col4a3 knockout mice when compared to wildtype littermates. Treatment with HPβCD significantly reduces fibrosis in Col4a3 knockout mice. *p<0.05, **p<0.01, One-Way ANOVA. **(H-J)** Representative transmission electron micrograph **(H)** and bar graph analysis of foot process effacement (yellow arrows) **(I)** and glomerular basement membrane thickness (GBM; yellow asterisk) **(J)** in wildtype and Col4a3 knockout mice treated with normal saline (NS) and HPβCD (CD). **(K)** Kaplan-Meier mortality curve showing that HPβCD treatment extends the lifespan of Col4a3 knockout mice compared to vehicle treated mice.

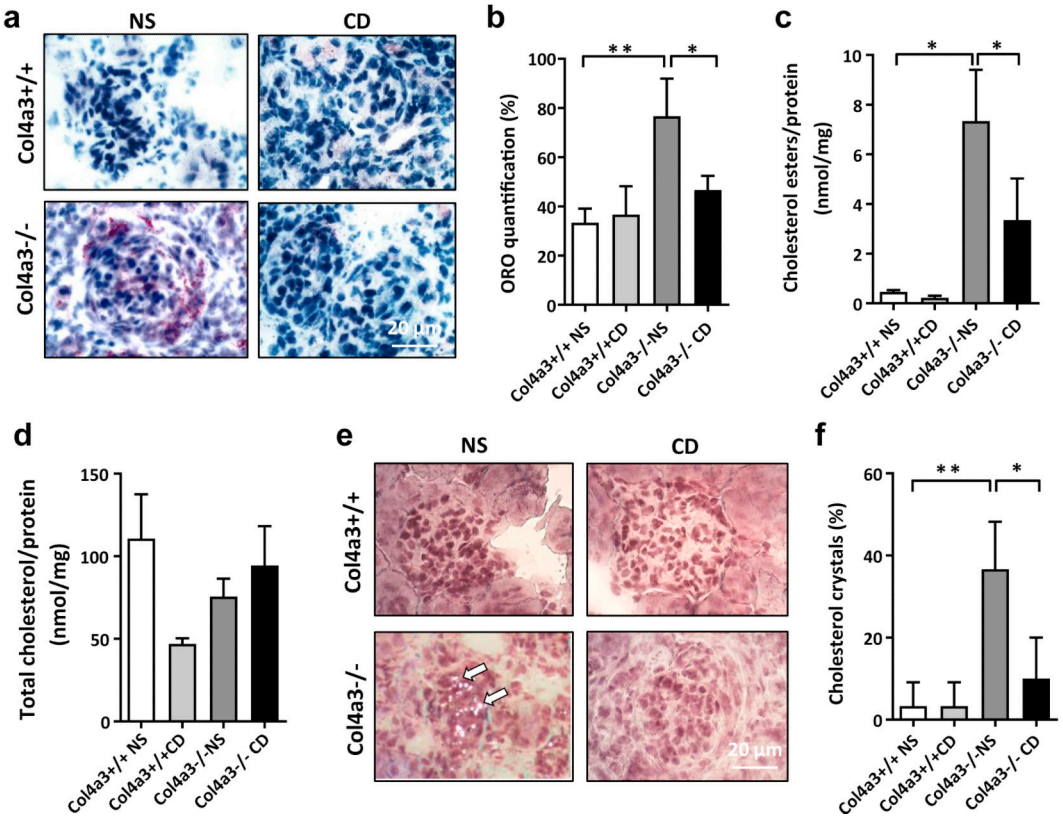

Figure 3. Effect of HPβCD on cholesterol homeostasis in Col4a3 knockout mice.

(A, B) Representative oil red O (ORO) staining of kidney sections (4 μm) **(A)** and bar graph analysis **(B)** from wildtype mice treated with normal saline (Col4a3+/+ NS) or cyclodextrin (Col4a3+/+ CD) and Col4a3 knockout mice treated with normal saline (Col4a3−/− NS) or HPβCD (Col4a3−/− CD) (40x). Bars are 20μm. *p<0.05, **p<0.01, One-way ANOVA. **(C)** Bar graph analysis showing significant reduction of cholesterol esters accumulation in Col4a3 knockout mice after 4 weeks of HPβCD treatment. *p<0.05, One-way ANOVA. **(D)** Bar graph analysis showing that HPβCD treatment does not affect total cholesterol levels in kidney cortexes of Col4a3 knockout mice when compared to wild type littermates. **(E, F)** Cholesterol crystal staining **(E)** and bar graph analysis **(F)** indicating significant cholesterol crystal accumulation in Col4a3 knockout mice compared to wild type littermates. HPβCD treatment leads to significant reduction in cholesterol crystals in Col4a3 knockout mice. Bars are 20μm. *p<0.05, **p<0.01, One-Way ANOVA. All data are presented as mean ± SD.

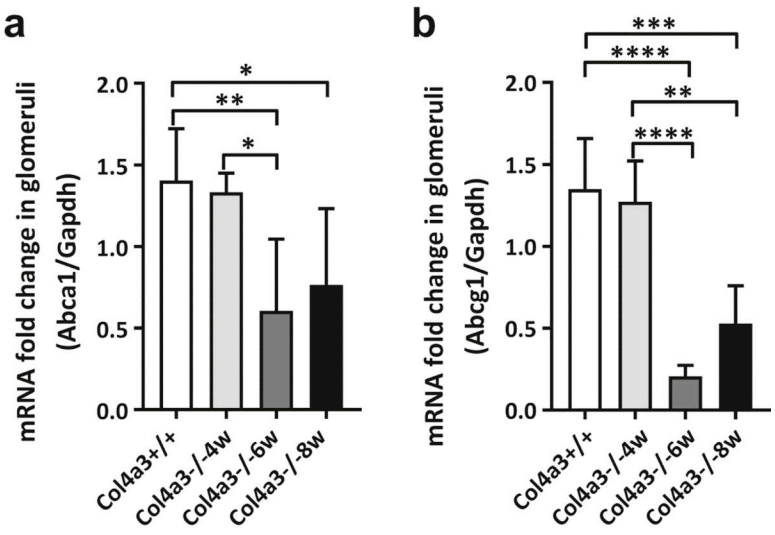

Figure 4. Analysis of Abca1 and Abcg1 gene expression in glomeruli of Col4a3 knockout mice.

(A) Quantitative real time PCR analysis of Abca1 expression in glomeruli isolated from 4, 6 and 8 week old Col4a3 knockout (Col4a3−/−) mice and 4 week old wildtype mice (Col4a3 +/+). *p<0.05, **p<0.01, One-Way ANOVA. **(B)** Quantitative real time PCR analysis of Abcg1 expression in glomeruli isolated from 4, 6 and 8 week old Col4a3 knockout (Col4a3−/−) mice and 4 week old wildtype mice (Col4a3 +/+). *p<0.05, **p<0.01, ***p<0.001, ****p<0.0001, One-Way ANOVA. All data are presented as mean ± SD.

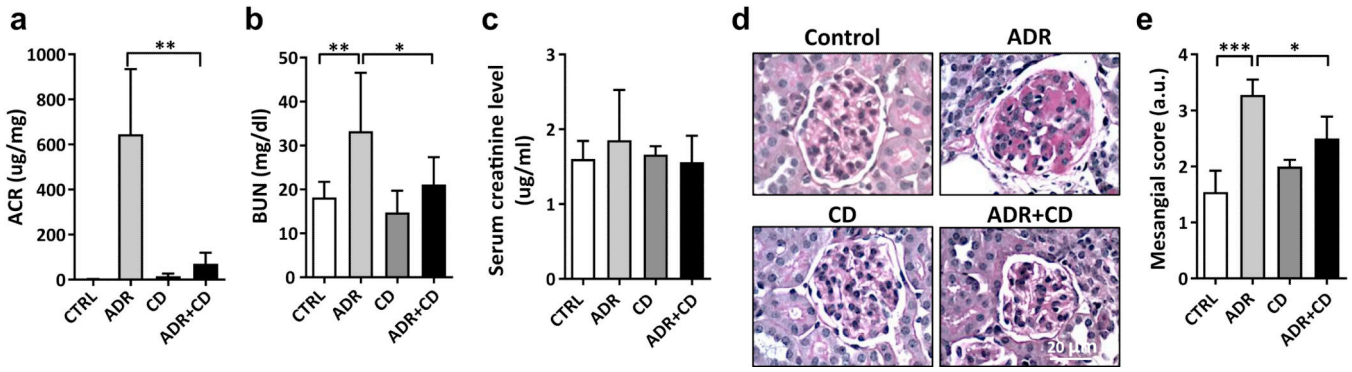

Figure 5. Hydroxypropyl-β–Cyclodextrin (HPβCD) improves renal function in Adriamycin (ADR) injected mice.

Four groups of BALB/c female mice (n=6 per group) were utilized: 1) Control (CTRL); 2) ADR, mice injected with a single dose of ADR (11 mg/kg); 3) CD, mice receiving only HPβCD subcutaneously (40 mg/kg); 4) ADR+CD, mice receiving HPβCD subcutaneously (40 mg/kg) after a single dose of ADR (11 mg/kg). All data are presented as mean ± SD. **(A)** HPβCD administration after a single dose of ADR results in a significant reduction in the albumin/creatinine ratio (ACR) 10 weeks after initiation of the treatment compared to untreated mice (CTRL). **p<0.01, One-Way ANOVA. **(B)** Bar graph analysis showing significantly increased serum BUN levels in ADR mice compared to controls. Treatment with HPβCD results in a significant reduction of serum BUN levels in the ADR+CD group compared to ADR group. *p<0.05; **p<0.01, One-Way ANOVA. **(C)** Serum creatinine did not increase in ADR-treated mice and was not affected by HPβCD. **(D)** Representative Periodic Acid-Schiff staining of kidney sections (4 μm) from CTRL, ADR, CD and ADR +CD mice after 10 weeks of treatment with HPβCD (40x). Bars are 20μm. **(E)** Bar graph analysis of the mesangial expansion scored by two blinded, independent investigators in PAS-stained kidney sections after 10 weeks of treatment with HPβCD. Treatment with HPβCD protects ADR injected mice from mesangial expansion. *p<0.05, ***p<0.001, One-Way ANOVA.

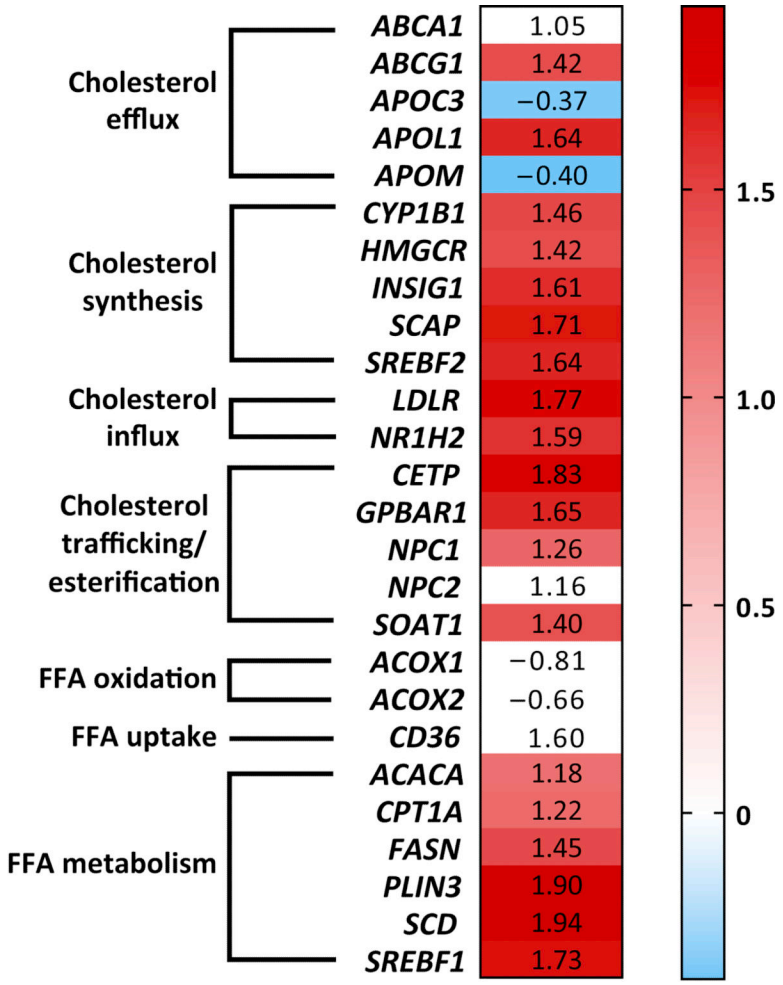

Figure 6. Microarray analysis of genes important in regulating lipid homeostasis using mRNA isolated from glomeruli of patients with FSGS enrolled in NEPTUNE study.

Microarray analysis of the glomerular transcripts in patients with FSGS enrolled in the NEPTUNE study. Numbers reflect fold change in glomerular gene expression in patients with FSGS when compared to living donors. Genes that passed FDR correction ($q \leq 0.05$) for multiple testing were considered significantly regulated and highlighted in blue (decreased expression) or red (increased expression) background colors. Genes that are not expressed in glomeruli from patients with FSGS are highlighted in white color.

Gene abbreviations: *ABCA1* – ATP-binding cassette subfamily A member 1; *ABCG1* – ATP-binding cassette subfamily G member 1; *ACACA* – acetyl-CoA carboxylase alpha; *ACOX1, ACOX2* – acyl-CoA oxidase 1 and 2, respectively; *APOC3* – apolipoprotein C3; *APOL1* – apolipoprotein L1; *APOM* – apolipoprotein M; *CD36* – cluster of differentiation 36; *CETP* – cholesteryl ester transfer protein; *CPT1A* – carnitine palmitoyltransferase I; *CYP1B1* – cytochrome P450 family 1 subfamily B member 1; *FASN* – fatty acid synthase; *GPBAR1* – G protein-coupled bile acid receptor 1; *HMGCR* – HMG-CoA reductase; *INSIG1* – insulin induced gene 1; *LDLR* – low density lipoprotein receptor; *NPC1 and NPC2* – Niemann-Pick disease, intracellular cholesterol transporter type 1 and type 2, respectively; *NR1H2* – nuclear receptor subfamily 1, group H, member 2; *PLIN3* – perilipin

3; *SCAP* – sterol regulatory element-binding protein cleavage-activating protein; *SCD* – stearoyl-CoA desaturase 1; *SOAT1* – sterol O-acetyltransferase 1; *SREBF1* – sterol regulatory element binding transcription factor 1; *SREBF2* – sterol regulatory element binding transcription factor 2.

Table 1.

Serology of ADR injected and Col4a3 knockout mice.

	FSGS				Alport syndrome			
	CTRL	**ADR**	**CD**	**ADR+CD**	**Col4a3+/+ NS**	**Col4a3+/+ CD**	**Col4a3−/− NS**	**Col4a3−/− CD**
Cholesterol, mg/dL	92.7±2.7	113.2±14.7	89.8±0.3	120.3±13.0$^{\&}$	117.9±3.4	131.3±4.7	203.5±10.0***	145.5±7.6**
HDL mg/dL	51.7±22.4	98.2±17.1	57.0±10.4	112.0±12.3	129.8±6.7	137.0±6.1	162.8±6.7$^{\#}$	138.3±5.4*
LDL mg/dL	BDL	−5.0±3.7	BDL	−3.3±0.5	5.4±0.3	5.8±0.9	14.9±1.2$^{\#}$	10.0±2.0
Triglycerides mg/dL	46.7±15.5	83.0±8.6	54.0±5.0	58.3±3.8	61.6±2.9	63.0±2.8	81.6±6.6	98.3±17.0
VLDL mg/dL	12.0±2.0	15.4±1.9	11.0±1.1	11.7±0.9	14.6±1.4	16.0±1.4	13.7±1.0	19.8±3.5*

Data are mean ± SD. ADR – adriamycin; CD – 2-hydroxypropyl-β-cyclodextrin (HPβCD); CTRL – control; NS – normal saline solution; HDL – high density lipids, LDL – low density lipids; VLDL – very low density lipids; BDL – below detection level.

* p<0.05

** p<0.01, when comparing CD treated vs. non-treated

$^{\#}$ p<0.01

*** p<0.001, when comparing knockout vs. controls

$^{\&}$ p<0.05, when comparing ADR+CD vs. CD group.